BIOCHEMISTRY
including biophysical chemistry & molecular biology

Article

pubs.acs.org/biochemistry

Complexes of Dual-Function Hemoglobin/Dehaloperoxidase with Substrate 2,4,6-Trichlorophenol Are Inhibitory and Indicate Binding of Halophenol to Compound I

Chunxue Wang,[†] Leslie L. Lovelace,[†] Shengfang Sun,[†] John H. Dawson,*[,†,‡] and Lukasz Lebioda*[,†,§]

[†]Department of Chemistry and Biochemistry, University of South Carolina, Columbia, South Carolina 29208, United States
[‡]School of Medicine, University of South Carolina, Columbia, South Carolina 29209, United States
[§]Center for Colon Cancer Research, University of South Carolina, Columbia, South Carolina 29209, United States

Supporting Information

ABSTRACT: The hemoglobin of sea worm *Amphitrite ornata*, which for historical reasons is abbreviated as DHP for dehaloperoxidase, has two physiological functions: it binds dioxygen in the ferrous state and dehalogenates halophenols, such as 2,4,6-trichlorophenol (TCP), using hydrogen peroxide as the oxidant in the ferric state. The crystal structures of three DHP variants (Y34N, Y34N/S91G, and L100F) with TCP bound show two mutually exclusive modes of substrate binding. One of them, the internal site, is deep inside the distal pocket with the phenolic OH moiety forming a hydrogen bond to the water molecule coordinated to the heme Fe. In this complex, the distal histidine is predominantly located in the closed position and also forms a hydrogen bond to the phenolic hydroxide. The second mode of TCP binding is external, at the heme edge, with the halophenol molecule forming a lid covering the entrance to the distal cavity. The distal histidine is in the open position and forms a hydrogen bond to the OH group of TCP, which also hydrogen bonds to the hydroxyl of Tyr38. The distance between the Cl4 atom of TCP and the heme Fe is 3.9 Å (nonbonding). In both complexes, TCP molecules prevent the approach of hydrogen peroxide to the heme, indicating that the complexes are inhibitory and implying that the substrates must bind in an ordered fashion: hydrogen peroxide first and TCP second. Kinetic studies confirmed the inhibition of DHP by high concentrations of TCP. The external binding mode may resemble the interaction of TCP with Compound I, the catalytic intermediate to which halophenols bind. The measured values of the apparent K_m for TCP were in the range of 0.3−0.8 mM, much lower than the concentrations required to observe TCP binding in crystals. This indicates that during catalysis TCP binds to Compound I. Mutant F21W, which likely has the internal TCP binding site blocked, has ∼7% of the activity of wild-type DHP.

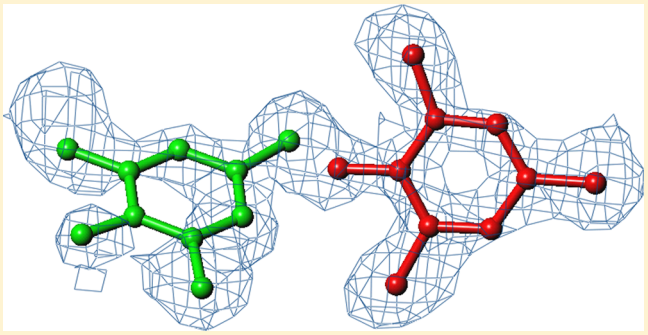

Amphitrite ornata is a sea worm that because of its appearance was named after the Greek goddess Amphitrite, the gorgeous wife of Poseidon. Its main body buried in mud is red, with white tentacles that extend into the water to catch food. The red color is due to coelomic hemoglobin, which is its most abundant protein. *A. ornata* co-inhabits estuarine mud flats with other polychaete worms, such as *Notomatus lobatus*, and hemichordata, such as *Saccoglossus kowalewskii*, which produce and secrete bromophenols presumably to repel predators and competing species. It has been proposed that to survive in such a toxic environment, the ancestral coelomic hemoglobin of *A. ornata* evolved to have, in addition to its dioxygen binding function, a dehaloperoxidase (DHP) functionality that neutralizes the poisonous bromophenols.[1] As a dehaloperoxidase, DHP has a relatively broad specificity, and although its physiological substrates are mainly bromophenols, it can oxidize a number of other haloaromatics according to Scheme 1.[2]

Scheme 1. Reaction Catalyzed by DHP

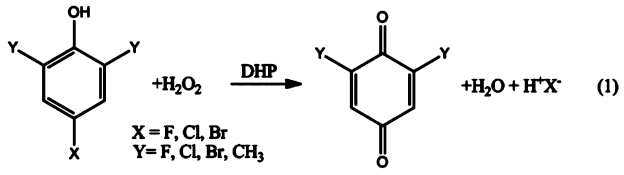

Other globins like hemoglobin and myoglobin from vertebrates, whose physiological role is limited to oxygen binding, also have some peroxidase activity in the ferric state, but that activity is lower by a factor in the range of 10−20, depending on the substrate.[3−5] On the other hand, specialized peroxidases, such as horseradish peroxidase, catalyze the

Received: May 17, 2013
Revised: August 15, 2013
Published: August 16, 2013

dx.doi.org/10.1021/bi400627w | *Biochemistry* 2013, 52, 6203−6210

Table 1. Crystallographic Data and Refinement Statistics[a]

	Y34N·TCP (PDB entry 4kmw)	Y34N/S91G·TCP (PDB entry 4kn3)	L100F·TCP (PDB entry 4kmv)
X-ray source	APS SER-CAT ID	APS SER-CAT ID	APS SER-CAT ID
wavelength (Å)	1.0000	1.000	1.000
no. of frames	140	75	180
oscillation range (deg)	1.0	1.0	1.0
temperature (K)	100	100	100
space group	$P2_12_12_1$	$P2_12_12_1$	$P2_12_12_1$
unit cell dimensions	58.553	58.982	58.539
a (Å)			
b (Å)	67.259	67.657	67.804
c (Å)	67.890	67.870	68.368
volume (Å^3)	267365	270840	271360
mosaicity (deg)	0.80	0.40	0.49
resolution range (Å)	47.8−1.79 (1.82−1.79)	44.5−1.78 (1.81−1.78)	4.78−1.44 (1.46−1.44)
redundancy	5.4 (4.0)	3.0 (2.7)	3.6 (1.9)
average $I/\sigma(I)$	13.4	20.2	14.4
total no. of reflections	140011	140586	332066
no. of unique reflections	25737	26181	49456
completeness (%)	98.9 (91.8)	98.8 (97.9)	98.3 (72.0)
total linear R_{merge}	7.9 (49.0)	4.0 (11.1)	5.4 (54.0)
R value (%), aniso	14.6 (23.8)	13.3 (14.0)	13.3 (25.9)
R value (%), iso	19.0 (29.6)	18.3 (22.2)	18.1 (32.9)
R_{free} (%)	23.8 (34.7)	21.4 (25.6)	20.1 (35.5)
	23.6 (32.9)	23.7 (30.1)	22.7 (37.0)
Ramachandran statistics (% of residues)			
most favored regions	94.4	94.0	92.9
additional allowed regions	5.6	6.0	6.3
generously allowed regions	0	0	0.8
average *B* factor for protein	27.7	24.3	22.2
average *B* factor for solvent	35.7	31.0	36.6

[a]Data in parentheses are for the highest-resolution shell.

dehaloperoxidase reaction faster than DHP by >1 order of magnitude.[6] Thus, the DHP catalytic efficiency is between those of classical globins and peroxidases with a His-ligated active site that is more globin-like than typical peroxidases.[7,8] The dioxygen binding function is universal and much older, 1.8 billion years,[9] than the emergence of polychaete in the Middle Cambrian ~530 million years ago.[10] Thus, the contemporary DHP evolved from an ancestral oxygen carrier as environmental pressures led to the evolution of its dehaloperoxidase activity and the emergence of its physiologically relevant dual function.

Two genes (*dhpA* and *dhpB*) present in *A. ornata* encode two isoproteins, DHP A and DHP B, respectively, each 137 amino acids long, which are different in only five amino acids.[11] Among those differences, Y34N is the closest to the heme, S91G is in the loop that contains the proximal histidine, His89, and other differences, I9L, R32K, and N81S, are more conservative and placed farther from the heme. The studies reported here of the Y34N variant of DHP and the Y34N/S91G double mutant were undertaken to identify the contribution of these variations to the functional differences observed between DHP A and DHP B.[12] The L100F mutant was designed to partially block the interior of the distal cavity.[13] While the physiological substrates of DHP are mostly bromophenols, the protein has been considered for bioremediation of sites polluted with anthropogenic 2,4,6-trichlorophenol (TCP). Also, TCP is more soluble than bromophenols and has often been used in kinetic and spectroscopic studies, although its apparent K_m value has not been reported. This report is the first crystallographic study of TCP complexes.

MATERIALS AND METHODS

Construction of the Native DHP Plasmid. The native DHP plasmid was generated from the pET-16b plasmid containing the gene of six-His-tagged DHP A and a unique NcoI site at the 5′-terminus. To remove the six-His tag, the second NcoI site was introduced by using a mutagenesis primer with a CCACCACCACCCCATGGGGTT sequence (5′ → 3′) and its reverse complement. The new plasmid incorporated two NcoI sites and was doubly digested with NcoI. Subsequently, it was ligated with T4 ligase followed by transformation into DH10*β* cells.

Site-Directed Mutagenesis. The DHP mutants were generated using the QuickChange method. The mutagenic primers were designed to be complementary to wild-type DHP cDNA around the site where the mutation was introduced. The desired DHP mutations were confirmed by LiCor DNA sequence analysis of the entire DHP gene (Engencore Laboratory, University of South Carolina).

Expression of DHP in Rosetta(DE3)pLysS. The pET-16b plasmid containing the gene encoding the Y34N DHP mutant was transformed into the Rosetta(DE3)pLysS competent cells and subsequently plated on agar plates with 30 *μ*g/mL chloramphenicol and 100 *μ*g/mL ampicillin. The cell cultures were inoculated in 2×YT medium with the proper antibiotics at 37 °C. When the OD_{600} reached 0.6, the temperature was decreased to 30 °C and isopropyl thiogalactopyranoside was

dx.doi.org/10.1021/bi400627w | *Biochemistry* 2013, 52, 6203−6210

added to a final concentration of 2 mM to induce DHP expression. The cells were kept at 30 °C overnight, pelleted by centrifugation, and stored at −80 °C.

Purification of Six-His-Labeled DHP and Native DHP. Purification of the His-tagged DHP mutants was conducted with established protocols, and all the kinetic studies were performed using His-tagged DHPs.[13,14] Recombinant native DHP mutants were purified as previously described with minor modifications.[15] A 25 g cell pellet was thawed and suspended in 100 mL of lysis buffer [20 mM Tris (pH 8.0) and 1 mM EDTA]. Lysozyme, DNase, RNase, and dithiothreitol were separately added to final concentrations of 1 mg/mL, 15 μg/mL, 50 μg/mL, and 0.5 mM, respectively. After incubation for 45 min at 4 °C, the mixture was mildly sonicated with duty cycle 90% and output 6 (seven cycles of 30 s bursts and four approximately 5 min intervals). Subsequently, cell debris was removed by centrifugation for 40 min at 14000 rpm. The reddish brown supernatant was subjected to ammonium sulfate fractionations. DHP was precipitated from 55 to 95% ammonium sulfate and then recovered by centrifugation. The precipitant was resuspended in 20 mM Tris (pH 8.0). The solution was dialyzed against 4 L of the same buffer to remove ammonium sulfate and then dialyzed against 4 L of 20 mM sodium phosphate (pH 5.0). After precipitated contaminants had been removed by centrifugation, the solution was applied to a SP-Sepharose fast flow cation exchange column, which was equilibrated with sodium phosphate (pH 5.0). The protein was eluted using a NaCl gradient from 0 to 0.5 M in sodium phosphate buffer (pH 5.0). Its purity was analyzed using UV−vis absorption spectroscopy by calculating the ratio of the heme absorbance at the Soret peak (406 nm) to the protein absorbance at 280 nm. The fractions with ratios greater than 2.5 were collected and concentrated to be further purified using a Sephacryl S-200 column with sodium phosphate buffer (pH 5.0). The fractions with ratios greater than 3.2 were considered to be pure and were pooled and concentrated. Subsequently, the buffer was exchanged with 20 mM sodium cacodylate (pH 6.5).

DHP in the ferric state was prepared by treating the purified protein with a small amount of potassium ferricyanide. The excess ferricyanide was removed using a Bio-Gel P-6 DG Desalting Gel gel-filtration column in the same buffer.[13,16,17]

Crystallization and Crystal Soaking. The Y34N variant of DHP was crystallized in both ferrous and ferric forms using the vapor diffusion method in a hanging-drop setup. The protein dissolved in 20 mM sodium cacodylate (pH 6.5) was concentrated to 10 mg/mL. The crystals were grown from solutions containing 0.2 M ammonium sulfate and 26−34% polyethylene glycol 4000, as previously reported.[15,18−21]

For the substrate binding experiments, solid TCP was dissolved in a 50% ethanol/water mixture. Subsequently, DHP crystals were soaked in an artificial 200 mM TCP mother liquor. The native and soaked crystals were briefly transferred to cryo-solutions, which additionally contained 20% ethylene glycol, and were flash-frozen in liquid nitrogen.

X-ray Diffraction Data Collection and Structure Determination. All data sets were collected at the SERCAT 22ID beamline at the Advanced Photon Source (APS) at Argonne National Laboratory (Argonne, IL). The data were indexed, integrated, and scaled with the HKL2000 software package.[22] Data collection and processing statistics are listed in Table 1. The structure of Y34N·TCP was determined using molecular replacement with Phaser[23] from the CCP4 suite of programs (CCP4, 1994) using the wild-type DHP (wt-DHP) structure [Protein Data Bank (PDB) entry 1EW6] as the initial model. For the subsequent analyses, the Y34N·TCP structure was used in molecular replacement. The resolution of the data is on the borderline for anisotropic treatment of *B* factors. R_{free} values are only slightly better, but *R* values are much lower for the anisotropic treatment. Statistics for both refinements are included in Table 1. The atomic coordinates resulting from both refinements are essentially the same. Structure rebuilding and refinements were performed using Turbo[24] and Refmac5,[25,26] respectively. Coordinates were superposed using LSQKAB[27] from the CCP4 suite. Figures 1−4 and Figure 1 and 3 of the Supporting Information were prepared using Turbo.

Dehaloperoxidase Activity Measurements. The dehaloperoxidase activity assay was performed on a Cary 400 spectrophotometer at 4 °C using a UV−vis absorption spectroscopy assay as described previously.[5,13,16,28] The 272 nm absorbance peak of the 2,4-dichloroquinone product was monitored versus time.[29] The initial rate for each reaction was calculated from the linear initial portion of the trace automatically using Cary Win UV set to kinetic mode. To measure the turnover number (k_{cat}), 150 μM TCP cosubstrate was mixed with DHP (1−3 μM enzyme) in 100 mM potassium phosphate buffer (pH 7), and then the reaction was initiated by varied concentrations of H_2O_2 (0−480 μM). To determine the K_m for TCP, varied concentrations of TCP (0.02−1.6 mM) were mixed with DHP, and then the reactions were initiated by addition of 160 μM H_2O_2. The initial rates as a function of H_2O_2 or TCP concentration were fit to the Michaelis−Menten equation using Prism version 5.

RESULTS

The crystal data and refinement parameters are listed in Table 1, while Table 2 presents a summary of ligands bound in the studied complexes.

Table 2. Ligands Bound in or at the Distal Cavity of DHP Mutants

	Y34N·TCP (PDB entry 4kmw)	Y34N/S91G·TCP (PDB entry 4kn3)	L100F·TCP (PDB entry 4kmv)
subunit A	TCP external	1/2 (TCP internal + H_2O)	1/2 (TCP internal + H_2O)
		1/2 TCP external	1/2 O_2
subunit B	TCP external	TCP external	H_2O + ethylene glycol

Structure of the Y34N·TCP Complex. After Y34N crystals had been soaked with TCP, the substrate bound in both subunits at the entrance to the distal cavity, creating a lid that closes the cavity entrance (Figure 1). We will refer below to this mode of binding as "external". TCP binding is accompanied by the distal histidine swinging out of the cavity and forming a strong hydrogen bond (2.5 Å) with the TCP hydroxyl that in turn forms another strong hydrogen bond (2.6 Å) with the hydroxyl of Tyr38. In addition to these hydrogen bonds, hydrophobic interactions formed with the heme and the side chains of Phe21, Phe35, Phe52, and Val59 stabilize TCP binding. Native Y34N crystallizes in the oxy-ferrous state, but the O_2 molecule was displaced upon TCP binding. However, there is no direct contact between the heme iron and the TCP molecule; the closest Fe neighbor is the Cl atom at position 4, but the observed distance of 3.4 Å is approximately 1 Å longer

dx.doi.org/10.1021/bi400627w | *Biochemistry* 2013, 52, 6203−6210

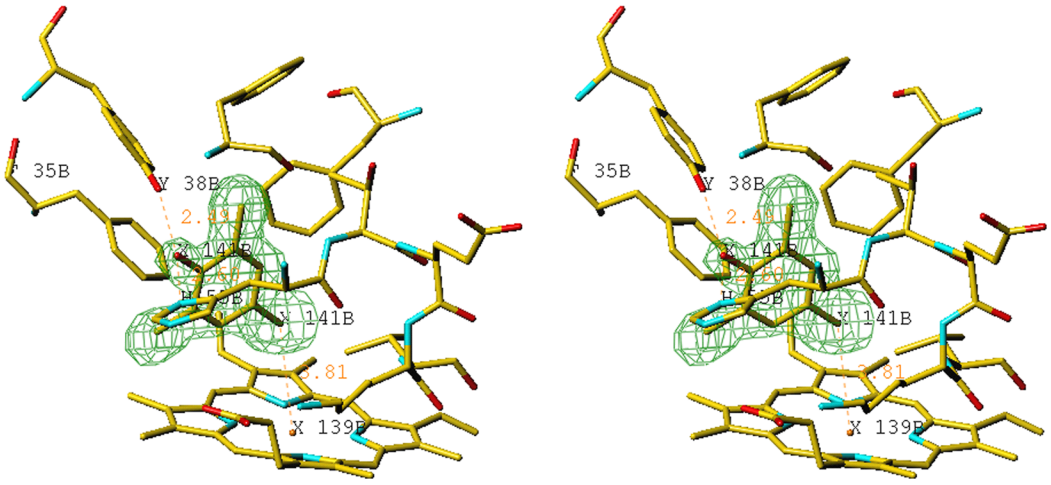

Figure 1. Stereoview of the electron density for TCP in the Y34N complex. The final $F_o - F_c$ omit map was contoured at the 2σ level. The hydroxyl of TCP forms two hydrogen bonds, one with Tyr38 and the other with the distal histidine, His55, which is swung out of the cavity.

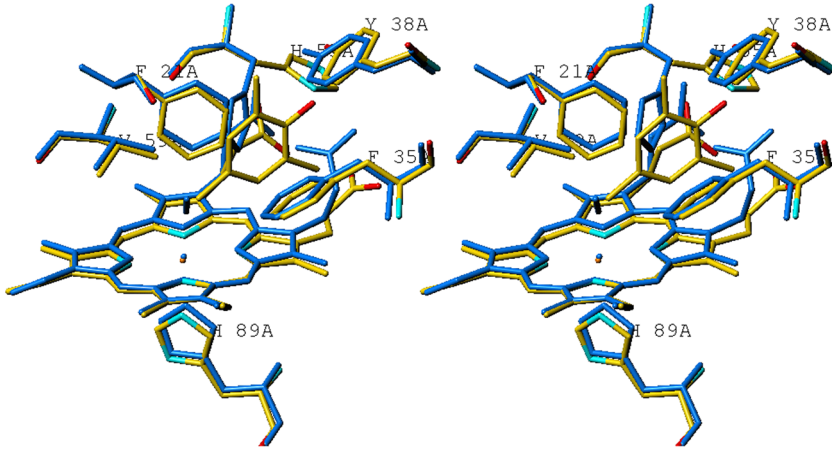

Figure 2. Stereoview of the least-squares superposition of Y34N complexes with oxygen (blue) and TCP (atom colors). The TCP molecule pushes the heme down, leading to its tilting. The Cl atom at position 4 is not in contact with the heme; its position is very close to that of the distal atom of the dioxygen molecule.

than the bonding distance. When the position of the Fe-coordinated O atom in the oxy-ferryl [Fe(IV)=O] complex is modeled, the distance between the ferryl O atom and Cl4 of TCP is 2.3 Å, ~0.8 Å shorter than the sum of their radii (Figure 1 of the Supporting Information). Thus, a TCP molecule, although not coordinating the heme iron, created steric hindrance that prevents bonding of water or peroxide molecules as a sixth ligand. Previous spectroscopic evidence of ferric DHP showed the transition from a six-coordinate high-spin state to a five-coordinate high-spin state upon TCP binding and thus indicated that the water molecule coordinated as the sixth ligand in the ferric DHP is also displaced.[12,30]

TCP binding resulted in a tilting of the heme by 6° and the movement of its edge by 0.8 Å (Figure 2). In both subunits, one of the heme propionates became disordered and the electron density for the loop of residues K87−S90, which contains the proximal histidine, His89, is poor when compared to those of other parts of the molecule and to the corresponding density in the Y34N·O_2 complex (to be published). Consistently, the *B* factors for the proximal histidine and its neighboring residues are much higher in the Y34N·TCP complex than in the Y34N·O_2 complex; they are shown in Figure 2 of the Supporting Information. This indicates that upon TCP binding, the loop of residues Lys87−Ser90 becomes more mobile and other conformations are populated. It appears that the loop mobility is induced by the heme movement. The standard conformation of this loop observed in the absence of TCP is unique for DHP; in other globins, the proximal histidine and its neighbors are a part of α-helix F.

Structure of the Y34N/S91G·TCP Complex. Soaking crystals of double mutant Y34N/S91G in a TCP solution led to a more complicated outcome. In subunit B, the TCP binding geometry is essentially the same as in the Y34N·TCP complex. However, in subunit A, two modes of TCP binding were observed with approximately equal occupancy (Figure 3 and Figure 3 of the Supporting Information). One mode is external, the same as in subunit B (and in the Y34N·TC complex). The other binding mode is entirely different, with the TCP deep in the distal cavity and the hydroxyl pointing toward the oxygen binding site of the heme. We will refer to this mode of binding as "internal". The binding in the internal and external sites cannot take place simultaneously because of steric hindrance; the distance between O1 of TCP in the internal site and Cl4 in the external site is 1.4 Å. Subunit B, which has a molecule of TCP bound in the external site, is similar to the analogous

dx.doi.org/10.1021/bi400627w | *Biochemistry* 2013, 52, 6203−6210

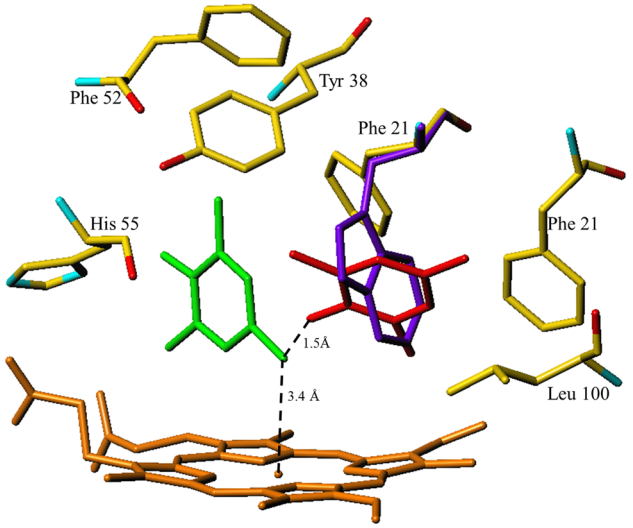

Figure 3. Distal cavity of subunit A in the structure of the Y34N/S91G·TCP complex and a modeled position for Trp21. DHP is shown in atom colors, and TCP bound in the external position is colored green and in the internal position red. The best modeled position of a tryptophan in F21W is colored violet.

Y34N·TCP complex with a tilted heme and a partially disordered proximal histidine loop. The half-occupancy of the two TCP sites in subunit A makes a detailed analysis of the conformational changes induced by ligand binding difficult.

Structures of the L100F·TCP Complex. Modeling suggested that the replacement of Leu100 with phenylalanine should block the internal TCP binding site. To check how the elimination of the internal TCP binding site affects the dehaloperoxidase activity of DHP, the L100F mutant was investigated. Previous kinetic studies showed that the rates of TCP dehalogenation by L100F are similar to those of wt-DHP.[13,31] The structure of L100F indeed confirmed the presence of steric hindrance.[31] However, the structure of L100F crystals soaked in TCP showed its binding, with ~50% occupancy, in the internal site of subunit A and a much lower occupancy in subunit B. The binding is allowed by conformational changes of Phe100, Phe60, and Phe21 shown in Figure 4. In the presence of TCP, there is a water molecule bound to the heme Fe, in its absence a dioxygen molecule. The

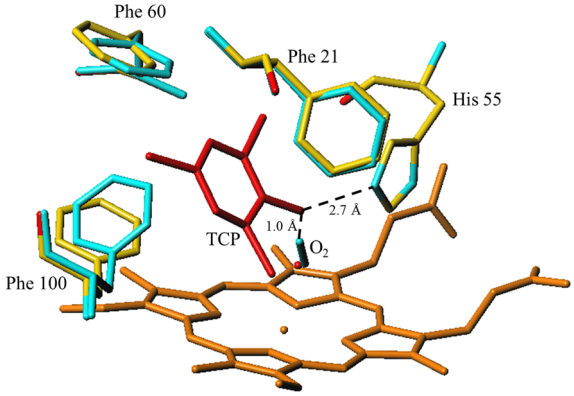

Figure 4. Distal cavity of the L100F·TCP complex in subunit A. The TCP molecule bound in the internal site is colored red. Phe21, Phe60, and Phe100 in the absence of bound TCP are colored cyan. The structure in the presence of TCP is shown in atom colors.

distal oxygen of O_2 is too close to the TCP hydroxyl to have both ligands present at the same time. The TCP binding in the internal site does not lead to the heme tilting and the disorder of the proximal histidine loop, which were observed upon TCP binding in the external site.

Subunit B has a water molecule coordinated to the heme iron; it is hydrogen bonded to a molecule of ethylene glycol present in the distal cavity, which originated from the cryo-solvent. The other hydroxyl of the ethylene glycol molecule forms a hydrogen bond to the hydroxyl of Tyr38. The distal His55 is outside the pocket and interacts with one of the heme propionates.

Dehaloperoxidase Activity of DHP Variants. DHP is unique among globins in having its proximal histidine located in a loop rather than being a part of a helix. It has been proposed that the increased flexibility and altered dynamics of this loop may contribute to its dehaloperoxidase activity.[35] The TCP binding in the external site indeed induced poor electron density and high *B* factors for this loop. To test if this increased loop mobility is indeed related to the dehaloperoxidase activity, we generated mutants of Lys87, the residue with the highest *B* factors. Conservative mutants Y34N/K87R and Y34N/K87S have approximately the same activity as Y34N, while Y34N/K87P, in which the presence of proline should restrict accessible conformations, had a slightly higher activity (Table 3). This would indicate that the variants have dynamics similar to that of wt-DHP and that the loop dynamics do not influence dehaloperoxidase activity.

Table 3. Activities of DHP and Its Variants[a]

	k_{cat} (min^{-1})
DHP A	26.1 ± 0.9
DHP Y34N/K87S	22.0 ± 1.0
DHP Y34N/K87R	22.3 ± 0.7
DHP Y34N/K87P	36.9 ± 0.9
DHP T56M	22.1 ± 1.0
DHP T56I	42.6 ± 1.1

[a]Data were measured at 150 μM TCP and varying H_2O_2 concentrations in 100 mM phosphate buffer (pH 7) at 4 °C.

The side chain of Thr56 forms a contact with the TCP molecule bound in the external site (CG2−Cl6 distance of 3.5 Å). Modeling suggested that mutations of Thr56 that introduce larger side chains may affect TCP binding. We have prepared such variants. T56M showed essentially the same activity as DHP A, and the activity of T56I was ~2-fold higher (Table 3).

Because L100F accommodated internal TCP binding, a less conservative F21W mutant was designed to block the internal TCP binding site. Modeling showed that all potential rotamers either block the TCP binding in the internal site or are disallowed because of steric hindrance. The best model is shown in Figure 3. Some adjustment in the distal cavity to accommodate its larger side chain must have taken place, and the mutant must have been expressed with standard yields. The mutant activity was only moderately lower, 7% of that of wt-DHP A (Table 4).

Kinetic studies of DHP and its variants as a function of TCP concentration yielded values of the apparent $3K_m$ that are listed in Table 4. They are in the TCP concentration range of 0.3−0.8 mM with the wild-type enzyme in the middle of the range, except for F21W, which has a K_m of 2.3 mM. In summary, none

dx.doi.org/10.1021/bi400627w | *Biochemistry* 2013, 52, 6203−6210

Table 4. Kinetic Studies of DHP Mutants[a]

	K_m^{TCP} (μM)	k_{cat}^{TCP} (min^{-1})	$k_{cat}^{H_2O_2}$ (min^{-1})	k_{cat}/K_m^{TCP} (mM^{-1} min^{-1})
DHP A	495 ± 62	63 ± 4	26.1 ± 0.9	127
Y34N	591 ± 76	85 ± 11	20.0 ± 0.6	143
T56M	828 ± 179	111 ± 14	22.1 ± 0.5	134
T56I	416 ± 72	111 ± 10	42.6 ± 1.2	267
Y38N	280 ± 94	119 ± 20	229 ± 8	425
F21W	2260 ± 512	19 ± 3	not determined	8.3

[a]In 150 μM TCP and varying H_2O_2 concentrations in 100 mM KP_i (pH 7) or in 160 μM H_2O_2 and varying TCP concentrations in 100 mM KP_i (pH 7).

of the mutations studied had a strong effect on the kinetic properties of DHP.

DISCUSSION

Two modes of binding of TCP to DHP have been observed: one site is internal, deep in the proximal cavity, while the other is external, forming a lid closing the distal cavity entrance. The internal binding mode is similar to that observed in the recently reported low-occupancy (~10%) complex of DHP A with an analogous substrate 2,4,6-tribromophenol (TBP).[32] The question that emerges is whether this is the productive mode of substrate binding as postulated by Zhao et al.[32] or just an opportunistic binding in the hydrophobic cavity. The answer to this question is crucial for our understanding of the mechanism of dehaloperoxidase catalysis employed by DHP. Two alternative mechanisms have recently been advanced. The first parallels the mechanism established for classical peroxidases.[33,34] In this mechanism, the reaction is initiated by H_2O_2 binding to form Compound I or Compound ES, which then abstracts a hydrogen atom (one electron and one protein) from the substrate generating a phenoxy radical, which dissociates from the enzyme. The phenoxy radical then either disproportionates to the product, or a second one-electron oxidation takes place with Compound II to yield the quinone product after reaction with water. Halophenol substrates interact with the heme edge, and their binding is transient.[33] The second mechanism, mostly advanced by Franzen and co-workers,[32] assumes that a halophenol molecule binds first in the distal cavity. This is followed by H_2O_2 binding and a single two-electron oxidation. Interaction of the oxidized intermediate with a water molecule leads to its dehalogenation and product release. The recently reported structure of the DHP·TBP complex with the TBP molecule bound in the internal site, analogous to the structure of the DHP·TCP complex reported here, was used to support the latter mechanism.[32]

The observation of an internal binding site was used to boost the mechanism advanced by Zhao et al.,[32] arguing that organic substrate binding is a necessary event. However, the Y34N/S91G·TCP and L100F·TCP structures reported here, which are more accurate than that of the DHP·TBP complex because the TCP occupancies are 50%, not 10% as observed for TBP, raise a number of issues. First, the TCP binding in the internal site is very capricious. The data presented in Tables 2 and 3 show that for DHP variants there is no correlation between their activity and the TCP binding mode and/or affinity observed in crystals. For some of the variants, two subunits present in the asymmetric part of the unit cell show different affinities and even different modes of binding. More consistency is expected for productive substrate binding, especially at concentrations 2 orders of magnitude higher than the K_m values. Importantly, the binding variability is not due to differences in diffusion through the crystals because in the isomorphic structures of the Y34N·TCP and Y34N/S91G·TCP complexes, the substrate (TCP) is present in both subunits with full occupancy.

Second, it was proposed that a water molecule that is ~10 Å from the C4 atom of TCP, the proposed site of nucleophilic attack, somehow migrates and interacts with the oxidized intermediate bound in the same site as the TCP substrate.[32] The migration of this water molecule is highly unlikely to take place as there is neither space at the C4 or Cl4 atom of TCP nor any indication suggesting the existence of a channel suitable for water molecule movement. Direct nucleophilic attack of the oxygen atom from Fe(IV)=O is also unlikely because the O−C4 distance (6.0 Å) is too long and the substrate position is unsuitable. Thus, the oxidized intermediate would have to leave the distal cavity for the final step of the reaction.

Third, simultaneous binding of O_2 and TCP in the distal cavity cannot take place because of steric hindrance; the positions of the phenolic O atom and the distal atom of O_2 are only 1.1 Å apart. Thus, in the presence of TCP in the distal cavity, a peroxide molecule cannot bind with a geometry similar to that of the dioxygen molecule. Neither is there an alternative, suitable binding geometry for peroxide, especially with the distal histidine present in the cavity. It is not likely that TCP bound in the internal site can shift in such a fashion that would allow hydrogen peroxide binding at the heme because of the size of the distal cavity. Also, the distal histidine forms a hydrogen bond with the TCP hydroxyl (Figure 4), and this interaction would have to be broken to allow H_2O_2 binding.

Finally, the F21W mutant, in which the internal TCP binding site must be entirely blocked, still has ~7% of the wt-DHP A activity. This is too much activity for a mechanism requiring occupancy of the internal binding site. These four entirely independent observations argue against internal TCP binding as a productive step in catalysis.

The structures of the Y34N and Y34N/S91G complexes with TCP revealed a novel TCP binding site, an external one. This binding mode must also be inhibitory because the TCP molecule blocks the entrance to the distal cavity and stabilizes the distal histidine in the catalytically inactive out position, thus disassembling the catalytic machinery for peroxide cleavage. Also, the Cl4 atom of TCP prevents the binding of even a water molecule to the heme iron let alone an H_2O_2 molecule. Spectroscopic data positively show that TCP binding leads to a five-coordinate Fe, indicating that in solution TCP binds in the external site.[12,30]

For classical peroxidases, the order of substrate binding and many aspects of their dehaloperoxidase mechanism, such as catalysis at the heme edge, are well established and likely similar to those of DHP.[33] The external binding mode observed in complexes of DHP with TCP may be related, though not closely similar, to the interaction between TCP and Compound I. In the absence of ligands, the distal histidine of DHP is observed in both the "in position" hydrogen bonded to the heme-iron ligand and in the "out position" outside the pocket;[35] its mobility is much higher than in other globins.[18] The oxygen atom bound to Fe(IV) in Compound I or Compound II is strongly polarized and thus a poor hydrogen bond acceptor; it is also farther from the distal histidine than a coordinated water molecule because the Fe−O bond is shorter. Thus, it appears that upon formation of Compound I the distal

dx.doi.org/10.1021/bi400627w | Biochemistry 2013, 52, 6203−6210

histidine loses its hydrogen bonding partner in the cavity, swings out into solvent, and is free to bind TCP and recruit it to the heme edge through the hydrogen bond observed in the complexes. Consequently, the affinity of DHP for TCP is higher upon activation of the enzyme by hydrogen peroxide. Previous studies of the inhibition of the myoglobin (Mb) dehaloperoxidative activity by phenol led to a similar conclusion: phenol, which acts as a competitive inhibitor, binds only after the activation of Mb by hydrogen peroxide.[16]

In addition to the hydrogen bond with the distal histidine (His55), the hydroxyl of Tyr38 forms a strong hydrogen bond to the hydroxyl of TCP; this appears to be an important contribution to the observed external binding mode. However, the replacement of Tyr38 with phenylalanine or asparagine, and thus elimination of this hydrogen bond, led to an increase in k_{cat} of 4- or 13-fold, respectively.[36] Our studies confirm the better catalytic efficiency of the Y38N variant. *A priori*, weaker substrate binding is not expected to cause increased activity or, in particular, a lower K_m. One possible explanation of this observation is that the observed complex with TCP in the external site is, as we argue, inhibitory, not the catalytic one. If one assumes that upon binding to Compound I the TCP molecule forms the hydrogen bonds observed in the inhibitory complex, it would approach the active oxygen with its Cl4 atom rather than C4. It may be suggested that the shorter side chain of Asn38 also forms a hydrogen bond with TCP that leads to a better geometry for the approach. We expressed non-His-tagged Y38N; however, the yield was low, and the protein did not crystallize.

The structural analyses and kinetic studies reported here strongly disagree with the model in which TCP binding takes place before hydrogen peroxide binding.[32] On the other hand, the data do not distinguish whether the reaction proceeds through two one-electron oxidation steps with the release of phenoxy radical intermediates or through one two-electron step producing benzoquinone. Interestingly, the establishment of the DHP mechanism will also help clarify the physiological role of DHP. So far, the DHP dehaloperoxidase activity has been considered to be crucial for halophenol detoxification. However, classical peroxidases producing dissociable radicals tend to be secretory and compartmentalized, while DHP functions in the worm coelom where radicals may be harmful. In plants, peroxidases are thought to produce phenoxy radicals to control the bacterial population.[37] A similar role of DHP as an activator of halophenols to augment their antibacterial properties should therefore also be considered.

CONCLUSION

Two alternative modes of binding of the TCP substrate to DHP have been observed. An internal TCP binding site is seen deep in the distal cavity partially blocking the dioxygen and, presumably, hydrogen peroxide binding side. An external TCP binding site has been found that overlaps with the position of the reactive oxygen atom in the DHP Compound I intermediate. Thus, both binding modes are inhibitory. Productive binding must occur via the Compound I state of DHP, implying ordered substrate binding: hydrogen peroxide first followed by halophenol. Several considerations lead us to project that the productive DHP binding mode may be similar to the external site reported here.

ASSOCIATED CONTENT

Supporting Information

A figure showing a comparison of inhibitory substrates binding in the distal cavity (TCP in the external mode and 4-IP) and their relation to the modeled position of the active oxygen in Compound I, a figure showing a comparison of the *B* factors in Y34N and the Y34N·TCP complex, a figure showing the electron density for TCP bound in the Y34N/S91G·TCP complex with one-half occupancy of the internal site and one-half occupancy of the external site, and Michaelis–Menten analysis of the kinetic data. This material is available free of charge via the Internet at http://pubs.acs.org.

Accession Codes

Coordinates and structure factors for DHP variants and their complexes have been deposited in the Protein Data Bank as entries 4kmw for the T34N·TCP complex, 4kn3 for the T34N/S91G·TCP complex, and 4kmv for the L100F·TCP complex.

AUTHOR INFORMATION

Corresponding Authors

*E-mail: lebioda@mailbox.sc.edu. Phone: (803) 777-2140.
*E-mail: jdawson@mailbox.sc.edu. Phone: (803) 777-7234.

Funding

This project was supported by the National Science Foundation (MCB 0820456).

Notes

The authors declare no competing financial interest.

ACKNOWLEDGMENTS

X-ray data were collected at the Southeast Regional Collaborative Access team (SER CAT) 22-ID beamline at the Advanced Photon Source (APS). Use of the APS is supported by the U.S. Department of Energy, Office of Science, under Contract W-31-109-Eng-38.

ABBREVIATIONS

DHP, dehaloperoxidase A from *A. ornata*; Y34N, Y34N/S91G, and L100F, mutants of DHP A; Mb, sperm whale myoglobin; TCP, 2,4,6-trichlorophenol; TBP, 2,4,6-tribromophenol; 4-IP, 4-iodophenol.

REFERENCES

(1) Lebioda, L., LaCount, M. W., Zhang, E., Chen, Y. P., Han, K., Whitton, M. M., Lincoln, D. E., and Woodin, S. A. (1999) An enzymatic globin from a marine worm. *Nature 401*, 445.

(2) Chen, Y. P., Woodin, S. A., Lincoln, D. E., and Lovell, C. R. (1996) An unusual dehalogenating peroxidase from the marine terebellid polychaete *Amphitrite ornata*. *J. Biol. Chem. 271*, 4609–4612.

(3) Osborne, R. L., Sumithran, S., Coggins, M. K., Chen, Y. P., Lincoln, D. E., and Dawson, J. H. (2006) Spectroscopic characterization of the ferric states of *Amphitrite ornata* dehaloperoxidase and *Notomastus lobatus* chloroperoxidase: His-ligated peroxidases with globin-like proximal and distal properties. *J. Inorg. Biochem. 100*, 1100–1108.

(4) Du, J., Sono, M., and Dawson, J. H. (2010) Functional switching of *Amphitrite ornata* dehaloperoxidase from O_2-binding globin to peroxidase enzyme facilitated by halophenol substrate and H_2O_2. *Biochemistry 49*, 6064–6069.

(5) Osborne, R. L., Coggins, M. K., Walla, M., and Dawson, J. H. (2007) Horse heart myoglobin catalyzes the H_2O_2-dependent oxidative dehalogenation of chlorophenols to DNA-binding radicals and quinones. *Biochemistry 46*, 9823–9829.

(6) Sumithran, S., Sono, M., Raner, G. M., and Dawson, J. H. (2012) Single turnover studies of oxidative halophenol dehalogenation by horseradish peroxidase reveal a mechanism involving two consecutive one electron steps: Toward a functional halophenol bioremediation catalyst. *J. Inorg. Biochem. 117*, 316−321.
(7) Roach, M. P., Chen, Y. P., Woodin, S. A., Lincoln, D. E., Lovell, C. R., and Dawson, J. H. (1997) *Notomastus lobatus* chloroperoxidase and *Amphitrite ornata* dehaloperoxidase both contain histidine as their proximal heme iron ligand. *Biochemistry 36*, 2197−2202.
(8) Franzen, S., Roach, M. P., Chen, Y. P., Dyer, R. B., Woodruff, W. H., and Dawson, J. H. (1998) The unusual reactivities of *Amphirite ornata* dehaloperoxidase and *Notomastus lobatus* chloroperoxidase do not arise from a histidine imidazolate proximal heme iron ligand. *J. Am. Chem. Soc. 120*, 4658−4661.
(9) Moens, L., Vanfleteren, J., Van de Peer, Y., Peeters, K., Kapp, O., Czeluzniak, J., Goodman, M., Blaxter, M., and Vinogradov, S. (1996) Globins in nonvertebrate species: Dispersal by horizontal gene transfer and evolution of the structure-function relationships. *Mol. Biol. Evol. 13*, 324−333.
(10) Morris, S. C. (1979) Middle Cambrian Polychaetes from the Burgess Shale of British-Columbia. *Philos. Trans. R. Soc., B 285*, 227.
(11) Han, K., Woodin, S. A., Lincoln, D. E., Fielman, K. T., and Ely, B. (2001) *Amphitrite ornata*, a marine worm, contains two dehaloperoxidase genes. *Mar. Biotechnol. 3*, 287−292.
(12) D'Antonio, J., D'Antonio, E. L., Thompson, M. K., Bowden, E. F., Franzen, S., Smirnova, T., and Ghiladi, R. A. (2010) Spectroscopic and mechanistic investigations of dehaloperoxidase B from *Amphitrite ornata*. *Biochemistry 49*, 6600−6616.
(13) Du, J., Huang, X., Sun, S., Wang, C., Lebioda, L., and Dawson, J. H. (2011) *Amphitrite ornata* dehaloperoxidase (DHP): Investigations of structural factors that influence the mechanism of halophenol dehalogenation using "peroxidase-like" myoglobin mutants and "myoglobin-like" DHP mutants. *Biochemistry 50*, 8172−8180.
(14) Belyea, J., Gilvey, L. B., Davis, M. F., Godek, M., Sit, T. L., Lommel, S. A., and Franzen, S. (2005) Enzyme function of the globin dehaloperoxidase from *Amphitrite ornata* is activated by substrate binding. *Biochemistry 44*, 15637−15644.
(15) de Serrano, V., Chen, Z., Davis, M. F., and Franzen, S. (2007) X-ray crystal structural analysis of the binding site in the ferric and oxyferrous forms of the recombinant heme dehaloperoxidase cloned from *Amphitrite ornata*. *Acta Crystallogr. D63*, 1094−1101.
(16) Huang, X., Wang, C., Celeste, L. R., Lovelace, L. L., Sun, S., Dawson, J. H., and Lebioda, L. (2012) Complex of myoglobin with phenol bound in a proximal cavity. *Acta Crystallogr. F68*, 1465−1471.
(17) Qin, J., Perera, R., Lovelace, L. L., Dawson, J. H., and Lebioda, L. (2006) Structures of thiolate- and carboxylate-ligated ferric H93G myoglobin: Models for cytochrome P450 and for oxyanion-bound heme proteins. *Biochemistry 45*, 3170−3177.
(18) Chen, Z., de Serrano, V., Betts, L., and Franzen, S. (2009) Distal histidine conformational flexibility in dehaloperoxidase from *Amphitrite ornata*. *Acta Crystallogr. D65*, 34−40.
(19) de Serrano, V., D'Antonio, J., Franzen, S., and Ghiladi, R. A. (2010) Structure of dehaloperoxidase B at 1.58 Å resolution and structural characterization of the AB dimer from *Amphitrite ornata*. *Acta Crystallogr. D66*, 529−538.
(20) de Serrano, V., and Franzen, S. (2013) Structural evidence for stabilization of inhibitor binding by a protein cavity in the dehaloperoxidase-hemoglobin from *Amphitrite ornata*. *Biopolymers 98*, 27−35.
(21) de Serrano, V. S., Davis, M. F., Gaff, J. F., Zhang, Q., Chen, Z., D'Antonio, E. L., Bowden, E. F., Rose, R., and Franzen, S. (2010) X-ray structure of the metcyano form of dehaloperoxidase from *Amphitrite ornata*: Evidence for photoreductive dissociation of the iron-cyanide bond. *Acta Crystallogr. D66*, 770−782.
(22) Otwinowski, Z., and Minor, W. (1997) Processing of X-ray diffraction data collected in oscillation mode. *Methods Enzymol. 276*, 307−326.
(23) Mccoy, A. J., Grosse-Kunstleve, R. W., Adams, P. D., Winn, M. D., Storoni, L. C., and Read, R. J. (2007) Phaser crystallographic software. *J. Appl. Crystallogr. 40*, 658−674.
(24) Roussel, A., and Cambillau, C. (1991) The Turbo-Frodo graphics package. In *Silicon graphics geometry partners directory*, p 81, Silicon Graphics, Mountain View, CA.
(25) Murshudov, G. N., Vagin, A. A., and Dodson, E. J. (1997) Refinement of macromolecular structures by the maximum-likelihood method. *Acta Crystallogr. D53*, 240−255.
(26) Murshudov, G. N., Skubak, P., Lebedev, A. A., Pannu, N. S., Steiner, R. A., Nicholls, R. A., Winn, M. D., Long, F., and Vagin, A. A. (2011) REFMAC5 for the refinement of macromolecular crystal structures. *Acta Crystallogr. D67*, 355−367.
(27) Kabsch, W., Kabsch, H., and Eisenberg, D. (1976) Packing in a New Crystalline Form of Glutamine Synthetase from *Escherichia coli*. *J. Mol. Biol. 100*, 283−291.
(28) Osborne, R. L., Taylor, L. O., Han, K. P., Ely, B., and Dawson, J. H. (2004) *Amphitrite ornata* dehaloperoxidase: Enhanced activity for the catalytically active globin using MCPBA. *Biochem. Biophys. Res. Commun. 324*, 1194−1198.
(29) Oberg, L. G., and Paul, K. G. (1985) The transformation of chlorophenols by lactoperoxidase. *Biochim. Biophys. Acta 842*, 30−38.
(30) Smirnova, T. I., Weber, R. T., Davis, M. F., and Franzen, S. (2008) Substrate binding triggers a switch in the iron coordination in dehaloperoxidase from *Amphitrite ornata*: HYSCORE experiments. *J. Am. Chem. Soc. 130*, 2128−2129.
(31) Plummer, A., Thompson, M. K., and Franzen, S. (2013) Role of polarity of the distal pocket in the control of inhibitor binding in dehaloperoxidase-hemoglobin. *Biochemistry 52*, 2218−2227.
(32) Zhao, J., de Serrano, V., Le, P., and Franzen, S. (2013) Structural and Kinetic Study of an Internal Substrate Binding Site in Dehaloperoxidase-Hemoglobin A from *Amphitrite ornata*. *Biochemistry 52*, 2427−2439.
(33) Osborne, R. L., Coggins, M. K., Raner, G. M., Walla, M., and Dawson, J. H. (2009) The mechanism of oxidative halophenol dehalogenation by *Amphitrite ornata* dehaloperoxidase is initiated by H_2O_2 binding and involves two consecutive one-electron steps: Role of ferryl intermediates. *Biochemistry 48*, 4231−4238.
(34) Poulos, T. L. (2010) Thirty years of heme peroxidase structural biology. *Arch. Biochem. Biophys. 500*, 3−12.
(35) LaCount, M. W., Zhang, E., Chen, Y. P., Han, K., Whitton, M. M., Lincoln, D. E., Woodin, S. A., and Lebioda, L. (2000) The crystal structure and amino acid sequence of dehaloperoxidase from *Amphitrite ornata* indicate common ancestry with globins. *J. Biol. Chem. 275*, 18712−18716.
(36) Franzen, S., Belyea, J., Gilvey, L. B., Davis, M. F., Chaudhary, C. E., Sit, T. L., and Lommel, S. A. (2006) Proximal cavity, distal histidine, and substrate hydrogen-bonding mutations modulate the activity of *Amphitrite ornata* dehaloperoxidase. *Biochemistry 45*, 9085−9094.
(37) Zipor, G., and Oren-Shamir, M. (2012) Do vacuolar peroxidases act as plant caretakers? *Plant Sci. 199−200*, 41−47.